A cosmographic analysis using DESI-DR2 and strong lensing: II. Distance Ratio measurements

Darshan Kumar,^a Deepak Jain,^b and Shobhit Mahajan,^c

^aInstitute for Gravitational Wave Astronomy, Henan Academy of Sciences, Zhengzhou 450046, Henan, China

 ${}^b\mathrm{Deen}$ Dayal Upadhyaya College, University of Delhi,

Dwarka, New Delhi 110078, India

 $^c\mathrm{Department}$ of Physics and Astrophysics, University of Delhi, Delhi 110007, India

E-mail: kumardarshan@hnas.ac.cn, djain@ddu.du.ac.in, sm@physics.du.ac.in

Abstract. The distance ratio derived from strong gravitational lensing systems, combined with complementary cosmological observations, offers a model-independent means to investigate the geometry and dynamics of the universe. In this study, we carry out a cosmographic investigation using the latest compilations of Type Ia supernovae (PantheonPlus, DESY5, and Union3), baryon acoustic oscillation measurements from DESI-DR2, and updated strong lensing distance ratios. The cosmographic series is expanded to fourth order in the variable y=z/(1+z) to constrain the deceleration, jerk, and snap parameters (q_0, j_0, s_0) . The analysis utilizes the distance sum rule (DSR) to provide an independent assessment of the spatial curvature parameter, Ω_{k0} , without assuming a specific dynamical model. Our results based on SGL distance ratio measurements combined with individual supernova datasets suggest a mild preference for an open universe, though a flat universe is supported at the 95% confidence level. Further, the inclusion of DESI-DR2 data in each combination provides tighter constraints on the parameters and confirms flatness within the 68% confidence level as expected in standard cosmology. The results for q_0 and j_0 are consistent with Λ CDM predictions across datasets, while the constraint on s_0 remains limited but improves with the inclusion of DESI-DR2. This is the second and final paper in a two-part series.

Keywords: Gravitational Lensing, Bayesian Reasoning, Baryon Acoustic Oscillations, Supernova Type Ia - Standard Candles.

C	ontents	
1	Introduction	1
2	Datasets and Methodology	3
	2.1 Strong Gravitational Lensing- Distance Ratio	3
	2.2 Late-Time Distance Probes: BAO and SNIa	4
	2.3 Methodology	5
3	Results	7
	3.1 Constraints without DESI-DR2	8
	3.2 Constraints with DESI-DR2	8
	3.3 Contour Analysis and Parameter Dependencies	9
4	Discussions and Conclusions	13

1 Introduction

The standard spatially flat Λ CDM model, which incorporates a cosmological constant and cold dark matter, successfully explains a wide range of cosmological observations. Nevertheless, unresolved tensions such as the Hubble constant discrepancy [1, 2], inconsistencies in the spatial curvature parameter [3, 4], and theoretical issues like fine-tuning and coincidence problems [5–7] persist. These challenges call for model-independent approaches that avoid assumptions tied to specific cosmologies.

The distance sum rule (DSR) has emerged as an effective tool to test spatial curvature without relying on background cosmological models, provided the universe adheres to the FLRW metric [8]. Previous works have applied the DSR with observations such as Type Ia supernovae, gamma-ray bursts, and gravitational-wave standard sirens [9–11]. For more details on the broader context of model-independent tests, we refer the reader to the introduction of the first paper in this series.

Strong gravitational lensing (SGL) systems provide a complementary observational probe that is sensitive to cosmic geometry through angular diameter distances [12]. Apart from their use in time-delay cosmography [13, 14], SGL also provides measurements of the distance ratio d_A^{ls}/d_A^{os} , where d_A^{ls} and d_A^{os} denote the angular diameter distances between the lens and the source, and between the observer and the source, respectively. These ratios can be used to study both the geometry of the universe and the mass distribution in lensing galaxies. Further, they can be used alongside other distance probes to constrain cosmological parameters without assuming a particular background model.

A central observable in SGL studies is the Einstein radius θ_E , which characterizes the angular size of the ring-like image formed when a source is aligned with a lens. The Einstein radius is a robust probe of the total projected mass of the lensing galaxy and, when combined with stellar kinematics, has been used to infer mass profiles and other galaxy properties [15–17]. Importantly, the observed angular size depends on the distance ratio d_A^{ls}/d_A^{os} ,

making it sensitive to the cosmological model assumed. Thus, by modeling lens galaxies and comparing theoretical predictions with observed Einstein radii, one can derive constraints on cosmological parameters [18–21].

The mass distribution within lens galaxies is a key factor in such analyses. The Singular Isothermal Sphere (SIS) profile, characterized by a mass density proportional to r^{-2} , offers a simple yet effective model for describing lens galaxies and is widely used in lensing studies. Further investigations have explored extended power-law models (EPL), in which the total mass density and luminous mass density follow $\rho_T(r) \propto r^{-\gamma}$ and $\rho_L(r) \propto r^{-\delta}$, respectively. These models describe how the mass distribution varies with radius and allow analysis to account for differences in both luminous and dark matter components within galaxies [22–27]. Such models have been applied to study galaxy evolution, structure formation, and important cosmological parameters [26, 28, 29]. By considering different and redshift dependent mass profiles, these models offer a more detailed description of galactic dynamics and interactions. At the same time, this approach introduces more parameters and modeling complexities, which increase uncertainties and present challenges for interpreting observational data.

In this analysis, we adopt the simpler SIS profile rather than extended models. Our objective is not to explore the detailed structure or evolution of lens galaxies, but rather to utilize distance ratio measurements as a clean geometrical probe to constrain cosmographic parameters and spatial curvature. By relying on the SIS model, we minimize assumptions about galaxy structure and focus on using lensing data to probe cosmic geometry in a model-independent framework.

Cosmography provides a model-independent framework to describe the kinematics of the universe's expansion without assuming any specific form for dark energy or gravity. By expanding observables such as the scale factor or luminosity distance as a Taylor series around the present epoch, cosmography directly relates measurable quantities to parameters like the Hubble constant (H_0) , the deceleration parameter (g_0) , the jerk parameter (j_0) , and higher derivatives that describe the evolution of cosmic expansion [30–32]. This approach relies only on the assumption of large-scale homogeneity and isotropy, as described by the FLRW metric, and avoids dependence on a particular cosmological model or dark energy parameterization. Despite its theoretical simplicity, standard expansions in redshift suffer from convergence issues at higher redshifts, typically beyond $z \approx 1$ [33, 34]. To extend its applicability, alternative redshift parametrizations such as y = z/(1+z) [35, 36] and rational approximations like Padé or Chebyshev polynomials have been introduced to ensure mathematical robustness across larger redshift domains [37, 38]. Cosmography has therefore become a powerful tool to constrain cosmic expansion and curvature independently. It provides an alternative to model-dependent analyses and offers a clear path for precision cosmology in the era of high-quality observational data.

In this work, we focus on the cosmographic analysis using SGL distance ratio measurements along with other distance probes, namely Type Ia supernova compilations (Pantheon-Plus, DESY5, and Union3) and baryon acoustic oscillation data from DESI-DR2. We expand the cosmographic series up to the fourth order in the variable y = z/(1+z) to constrain the deceleration, jerk, and snap parameters (q_0, j_0, s_0) , and we implement the DSR to probe spatial curvature Ω_{k0} independently. Compared to the first paper, which focused primarily

on time-delay distances, here we emphasize the use of distance ratios as an independent geometrical probe that provides an independent constraint on cosmic expansion and geometry.

The inclusion of SGL distance ratios in cosmographic analyses represents a novel approach. Previous studies either relied on distance ladder calibrations or assumed a flat universe, whereas this study applies the DSR framework directly to distance ratio measurements without such assumptions. By combining the largest available samples of SGL systems with supernova and BAO datasets, we offer a unique and robust way to investigate cosmic curvature and expansion. Our goal is to explore the consistency of these probes with standard cosmological predictions and to examine how their combination can enhance the reliability of cosmological constraints.

The structure of this paper is as follows. In Section 2, we describe the datasets and methodology used in this analysis. Section 3 presents the main results, including constraints on cosmographic and curvature parameters. Finally, Section 4 summarizes the conclusions and outlines potential directions for future research.

2 Datasets and Methodology

In this section, we describe the observational datasets used this analysis. We also explain the statistical approach based on Bayesian inference and Markov Chain Monte Carlo (MCMC) techniques, which we use to derive constraints on cosmological parameters.

2.1 Strong Gravitational Lensing- Distance Ratio

The Singular Isothermal Sphere (SIS) model remains a standard framework for studying galaxy-galaxy lensing due to its simplicity and physical relevance. In this model, the lensing galaxy is assumed to have a spherically symmetric mass distribution with a density profile that decreases as the inverse square of the radial distance, $\rho(r) \propto r^{-2}$. The spherical symmetry leads to the formation of two images of the background source. The Einstein radius in this model is expressed as [39, 40]

$$\theta_E = 4\pi \frac{\sigma_{v,\text{SIS}}^2}{c^2} \frac{d_A^{\text{ls}}}{d_A^{\text{os}}},\tag{2.1}$$

where $\sigma_{v,\rm SIS}$ represents the characteristic velocity dispersion of the lens galaxy. This parameter can be estimated through spectroscopic observations that measure the velocity dispersion within an aperture, denoted by $\sigma_{\rm ap}$. Since the observed dispersion depends on the aperture size, it requires rescaling to approximate the central velocity dispersion, $\sigma_{v,e/2}$, at the galaxy's half-light radius. The aperture $\theta_{\rm ap}$, originally measured using a rectangular slit, is converted into an equivalent circular aperture using the relation [41]

$$\theta_{\rm ap} \simeq 1.025 \times \sqrt{\frac{\theta_x \theta_y}{\pi}},$$
 (2.2)

where θ_x and θ_y are the slit dimensions. For uniformity across different observational setups, velocity dispersions are normalized to correspond to half the effective radius $\theta_{\text{eff}}/2$ using the aperture correction formula [41]:

$$\sigma_{v,\text{SIS}}^2 = \sigma_{e/2} = \sigma_{\text{ap}} \left(\frac{\theta_{\text{eff}}}{2\theta_{\text{ap}}} \right)^{\eta}.$$
 (2.3)

Here, we consider the value of the correction parameter $\eta = -0.066 \pm 0.035$ which is derived by Cappellari et al. [42]. This correction ensures that the velocity dispersion matches the scale of the Einstein radius and improves the accuracy of cosmological analyses using the SIS model.

In this analysis, we adopt a sample of galaxy-scale strong gravitational lensing systems originally compiled by Cao et al. (2015) [22] and subsequently refined by Chen et al. (2019) [26]. The sample consists of 161 lensing galaxies, primarily classified as early-type (E/S0 morphologies), carefully chosen to exclude systems with substantial substructures or nearby companions that could bias lensing measurements. This dataset integrates multiple surveys: 5 systems from the LSD survey [15, 16, 43, 44], 26 from the Strong Lenses in the Legacy Survey (SL2S) [45–48], 57 from the Sloan Lens ACS Survey (SLACS) [49–51], 38 from the "SLACS for the Masses" extension (S4TM) [52, 53], 21 from the BOSS Emission-Line Lens Survey (BELLS) [54], and 14 from the BELLS for GALaxy-Ly EmitteR sYstems survey (BELLS-GALLERY) [55, 56].

The sample provides detailed measurements necessary for distance ratio analyses, including the lens redshift (z_l) , source redshift (z_s) , Einstein radius (θ_E) , aperture velocity dispersion $(\sigma_{\rm ap})$ measured within an angular aperture $\theta_{\rm ap}$, and the half-light angular radius of the lens galaxy $(\theta_{\rm eff})$. The lenses span a redshift range of $0.0624 \le z_l \le 1.004$, while the source redshifts range from $0.197 \le z_s \le 3.595$. The angular Einstein radius, which depends on the distance ratio $d_{\rm A}^{\rm ls}/d_{\rm A}^{\rm os}$ between lens and source and observer and source, provides a robust geometric probe for testing cosmological models, provided an accurate lens model is adopted.

2.2 Late-Time Distance Probes: BAO and SNIa

In this analysis, we incorporate late-time distance probes from Baryon Acoustic Oscillations (BAO) and Type Ia supernovae (SNIa), which complement the strong lensing distance ratio measurements in constraining cosmological parameters. For a comprehensive description of these datasets, their construction, and associated systematics, we refer the reader to Paper I of this series.

• Baryon Acoustic Oscillations (BAO):

We utilize the second-year BAO dataset released by the Dark Energy Spectroscopic Instrument (DESI), corresponding to three years of observations [57, 58]. The dataset includes the full covariance matrix to account for correlations among distance indicators. The BAO observables are expressed as distance ratios normalized by the sound horizon at the drag epoch, namely $d_{co}(z)/r_d$, $d_H(z)/r_d$, and $d_V(z)/r_d$, which are sensitive to the cosmic expansion history and early universe physics [59–61]. In the BAO analysis, a strong degeneracy appears between the Hubble constant H_0 and the sound horizon r_d . To break this degeneracy, we apply a Gaussian prior on r_d using the values reported in reference [62].

• Type Ia Supernovae (SNIa):

For the supernova observations, we analyze three independent compilations: Pantheon-Plus [63], Union3 [64], and DESY5 [65]. The Pantheon-Plus dataset consists of 1701 light curves from 1550 spectroscopically confirmed SNIa spanning the redshift range

 $0.001 \le z \le 2.26$ [63]. To minimize the effects of peculiar velocities on the Hubble diagram, we exclude samples with $z \le 0.01$ and use 1590 light curves over 0.01 < z < 2.26, which have been carefully corrected for observational biases and cross-calibrated across multiple surveys [66–69]. Union3 provides 2087 supernovae, using Bayesian hierarchical modelling to address systematic uncertainties [64]. At present, only the binned distance modulus measurements are publicly available for this sample; accordingly, we restrict our analysis to these data points and incorporate their corresponding covariance matrix. The DESY5 sample, based on the full five-year Dark Energy Survey, contains 1635 photometrically classified supernovae in the redshift range 0.0596 < z < 1.12, along with 194 low-redshift supernovae from more recent surveys [65]. These datasets are treated separately in our analysis to avoid cross-correlations and to test the robustness of cosmological parameter estimates.

2.3 Methodology

• Cosmographic Framework

The cosmographic approach extracts information directly from observations by assuming only homogeneity and isotropy, without reference to a specific cosmological model. The metric is described by the FLRW line element:

$$ds^{2} = -c^{2}dt^{2} + a^{2}(t) \left[\frac{dr^{2}}{1 - kr^{2}} + r^{2}d\Omega^{2} \right],$$
 (2.4)

where c is the speed of light, k represents spatial curvature, and a(t) is the scale factor normalized to unity at the present time. The scale factor is expanded as a Taylor series around the present epoch:

$$\frac{a(t)}{a(t_0)} = 1 + H_0(t - t_0) - \frac{q_0}{2}H_0^2(t - t_0)^2 + \frac{j_0}{3!}H_0^3(t - t_0)^3 + \frac{s_0}{4!}H_0^4(t - t_0)^4 + \dots$$
 (2.5)

where the cosmographic parameters are defined as

$$H_0 = \frac{\dot{a}}{a}\Big|_{t=t_0}, \quad q_0 = -\frac{1}{H_0^2} \frac{\ddot{a}}{a}\Big|_{t=t_0}, \quad \dot{j}_0 = \frac{1}{H_0^3} \frac{\ddot{a}}{a}\Big|_{t=t_0}, \quad s_0 = \frac{1}{H_0^4} \frac{\ddot{a}}{a}\Big|_{t=t_0}. \tag{2.6}$$

To ensure convergence across a wide redshift range, we expand the Hubble parameter in terms of the variable $y = \frac{z}{1+z}$ as

$$H(y) = H_0 + \frac{dH}{dy}\Big|_{y=0} y + \frac{1}{2} \left. \frac{d^2H}{dy^2} \right|_{y=0} y^2 + \frac{1}{6} \left. \frac{d^3H}{dy^3} \right|_{y=0} y^3 + \dots$$
 (2.7)

The distances such as angular diameter distance d_A and comoving distance d_{co} can be expressed as functions of these cosmographic parameters. For details on the expansions and their application, we refer the reader to paper I.

• Distance Sum Rule (DSR)

The DSR provides a geometric relation among the dimensionless comoving distances between the observer, lens, and source, denoted as

$$D_{\text{co}}^{\text{os}} = \frac{H_0}{c} d_{\text{co}}^{\text{os}},$$

$$D_{\text{co}}^{\text{ol}} = \frac{H_0}{c} d_{\text{co}}^{\text{ol}},$$

$$D_{\text{co}}^{\text{ls}} = \frac{H_0}{c} d_{\text{co}}^{\text{ls}}.$$
(2.8)

In a flat universe, these distances satisfy $D_{\rm co}^{\rm os}=D_{\rm co}^{\rm ol}+D_{\rm co}^{\rm ls}$. For a non-flat universe, the relation generalizes to:

$$D_{\text{co}}^{\text{ls}} = D_{\text{co}}^{\text{os}} \sqrt{1 + \Omega_{k0} (D_{\text{co}}^{\text{ol}})^2} - D_{\text{co}}^{\text{ol}} \sqrt{1 + \Omega_{k0} (D_{\text{co}}^{\text{os}})^2}$$
(2.9)

Using the expression of DSR given in Equation 2.9, one can rewrite it in terms of distance ratio as

$$d_{\rm AR}^{\rm th} = \frac{d_A^{\rm ls}}{d_A^{\rm os}} = \frac{d_{\rm co}^{\rm ls}}{d_{\rm co}^{\rm os}} = \frac{D_{\rm co}^{\rm ls}}{D_{\rm co}^{\rm os}} = \sqrt{1 + \Omega_{k0} \left(D_{\rm co}^{\rm ol}\right)^2} - \frac{D_{\rm co}^{\rm ol}}{D_{\rm co}^{\rm os}} \sqrt{1 + \Omega_{k0} \left(D_{\rm co}^{\rm os}\right)^2}$$
(2.10)

This formulation allows direct determination of the curvature parameter Ω_{k0} from observations or cosmography expressions of $D_{\rm co}^{\rm ol}$ and $D_{\rm co}^{\rm os}$ without assuming a fiducial cosmological model. In this paper, we apply the DSR to distance ratio measurements. This approach complements the analysis of time-delay distances presented in paper I.

Chi-Square Formalism

• SGL Distance Ratio:

$$\chi_{\text{SGL}}^{2}(\Omega_{k0}, q_{0}, j_{0}, s_{0}) = \sum_{i} \left[\frac{d_{AR}^{\text{th}} - d_{AR}^{\text{obs}}}{\sigma_{d_{AR}^{\text{obs}}}} \right]^{2}$$
(2.11)

where d_{AR} represents the observed and theoretical distance ratios derived from the lensing systems.

Following Chen et al. [26], the total uncertainty in the velocity dispersion is given by

$$\left(\Delta \sigma_{\rm SIS}^{\rm tot}\right)^2 = \left(\Delta \sigma_{e/2}^{\rm stat}\right)^2 + \left(\Delta \sigma_{e/2}^{\rm AC}\right)^2 + \left(\Delta \sigma_{e/2}^{\rm sys}\right)^2,\tag{2.12}$$

where $\Delta \sigma_{e/2}^{\rm stat}$ denotes the statistical uncertainty from measurements, $\Delta \sigma_{e/2}^{\rm AC}$ represents the propagated uncertainty from the aperture correction to the half effective radius, and $\Delta \sigma_{e/2}^{\rm sys}$ accounts for systematic uncertainties.

The aperture correction uncertainty is computed as

$$\left(\Delta \sigma_{e/2}^{\rm AC}\right)^2 = (\Delta \sigma_{\rm ap})^2 \left(\frac{\theta_{\rm eff}}{2\theta_{\rm ap}}\right)^{2\eta} + \sigma_{\rm ap}^2 \left(\frac{\theta_{\rm eff}}{2\theta_{\rm ap}}\right)^{2\eta} \ln^2 \left(\frac{\theta_{\rm eff}}{2\theta_{\rm ap}}\right) (\Delta \eta)^2, \tag{2.13}$$

where $\theta_{\rm eff}$ and $\theta_{\rm ap}$ are the angular half-light and aperture radii respectively, and η is the aperture correction parameter.

For the systematic uncertainty, $\Delta \sigma_{e/2}^{\rm sys}$ reflects potential deviations arising from assumptions on the consistency between dynamical mass and Einstein mass. We adopt a 3% systematic uncertainty on the model-predicted velocity dispersion to account for line-of-sight matter effects, as suggested by Jiang & Kochanek [70].

• SNIa:

The theoretical apparent magnitude for SNIa is given by:

$$m^{\text{th}} = 5 \log_{10}(D_L) + \mathcal{M},$$
 (2.14)

where $\mathcal{M} = 5 \log_{10} \left(\frac{c}{H_0} \right) + M_B + 25$. In this analysis, we treat \mathcal{M} as a nuisance parameter and numerically marginalize over it using a wide prior distribution.

After marginalizing over \mathcal{M} , the chi-square for SNIa data is:

$$\chi_{\text{SNIa}}^2(\Omega_{k0}, q_0, j_0, s_0) = a - \frac{b^2}{f} + \ln\left(\frac{f}{2\pi}\right),$$
(2.15)

where a, b, and f are defined as $a = \Delta \bar{m}^T \text{Cov}^{-1} \Delta \bar{m}$, $b = \Delta \bar{m}^T \text{Cov}^{-1} I$, and $f = I^T \text{Cov}^{-1} I$. Here, $\Delta \bar{m} = m^{\text{obs}} - 5 \log_{10}(D_L)$, and I denotes a vector of ones (or the identity matrix in the covariance formalism). This form incorporates both statistical and systematic uncertainties. For a detailed derivation and discussion of the marginalization procedure, we refer the reader to Paper I.

• DESI-DR2: The Chi-square expression for this sample is given as

$$\chi_{\text{DESI}}^{2}(H_{0}, \Omega_{k0}, q_{0}, j_{0}, s_{0}) = [X_{\text{obs}} - X_{\text{th}}]^{T} \text{Cov}^{-1} [X_{\text{obs}} - X_{\text{th}}], \qquad (2.16)$$

where X corresponds to the set of distance observables normalized by the sound horizon.

• Joint Analysis:

$$\chi_{\text{Joint}}^2 = \chi_{\text{SGL}}^2 + \chi_{\text{SNIa}}^2 + \chi_{\text{DESI}}^2, \tag{2.17}$$

where χ^2_{SNIa} applies separately to the PantheonPlus, Union3, and DESY5 datasets.

For the cosmological parameters considered in this analysis, we adopt flat priors within specified ranges, as listed in Table 1. The exploration of the parameter space is performed using the Markov Chain Monte Carlo (MCMC) method implemented through the *emcee* sampler [71]. The sampler is configured with 12 walkers, each running for 10,000 steps to to achieve a thorough exploration of the posterior distribution. The initial 30% of samples are treated as the burn-in phase and excluded from the final analysis. The convergence of this sampler is monitored by computing the integrated auto-correlation time, τ_f , utilizing the *autocorr.integrated_time* function provided by the *emcee* package. This procedure helps guarantee that the chains have mixed well and the results are statistically robust.

3 Results

In this section, we present the constraints on cosmological and cosmographic parameters obtained from the combination of strong gravitational lensing with Type Ia supernova datasets and DESI-DR2 measurements. We analyse three different supernova samples, namely PantheonPlus, Union3, and DESY5, for cases without the inclusion of DESI-DR2 and with the inclusion of DESI-DR2. The estimated values for the Hubble constant (H_0) , spatial curvature parameter (Ω_{k0}) , deceleration parameter (q_0) , jerk parameter (j_0) , and snap parameter (s_0) are shown in Table 3. The joint posterior distributions and correlation matrices are shown in Figures 1, 2, and 3.

Parameter	Prior Range
$H_0 \ [{\rm km s^{-1} Mpc^{-1}}]$	$\mathbb{U}[0, 100]$
Ω_{k0}	$\mathbb{U}[-0.5, 1]$
q_0	$\mathbb{U}[-2,2]$
j_0	$\mathbb{U}[-3,3]$
s_0	$\mathbb{U}[-10, 10]$

Table 1: Flat priors assumed for the Hubble constant, spatial curvature, and cosmographic parameters.

3.1 Constraints without DESI-DR2

Table 3 presents the constraints from the SGL dataset combined with each supernova sample, excluding DESI-DR2. For the SGL+PantheonPlus combination, the curvature parameter is constrained as $\Omega_{k0} = 0.049^{+0.083}_{-0.077}$ which is consistent with a flat universe within the 68% confidence level. The deceleration parameter $q_0 = -0.472^{+0.073}_{-0.067}$ confirms cosmic acceleration with moderate precision. The jerk parameter $j_0 = 0.774^{+0.705}_{-0.737}$ overlaps with the standard model expectation, whereas the snap parameter $s_0 = -0.749^{+6.995}_{-6.395}$ remains largely unconstrained.

For the SGL+Union3 combination, the best fit value of Ω_{k0} i.e. $0.065^{+0.087}_{-0.082}$ shows a slight preference for an open universe but remains compatible with flat geometry at 68% confidence level. The deceleration parameter $q_0 = -0.272^{+0.151}_{-0.121}$ shows a weaker acceleration, while the jerk parameter $j_0 = -0.372^{+1.029}_{-1.196}$ shows broad uncertainties. The snap parameter $s_0 = -3.327^{+7.753}_{-4.832}$ is poorly constrained.

For the SGL+DESY5 dataset, the curvature is $\Omega_{k0}=-0.031^{+0.086}_{-0.075}$, consistent with flat universe at 68% confidence level. The deceleration parameter $q_0=-0.735^{+0.141}_{-0.135}$ suggests stronger acceleration. The jerk parameter $j_0=2.248^{+0.857}_{-0.933}$ indicates a possible deviation from unity, although the 95% confidence level interval includes unity. The snap parameter $s_0=-1.113^{+7.250}_{-6.240}$ remains unconstrained.

3.2 Constraints with DESI-DR2

The inclusion of DESI-DR2 considerably tightens the parameter constraints for all dataset combinations, as shown in Table 3. For SGL+PantheonPlus+DESI-DR2, the Hubble constant is determined as $H_0 = 67.859^{+0.469}_{-0.438} \text{ km s}^{-1} \text{ Mpc}^{-1}$, closely aligned with results from other cosmological probes. The curvature parameter tightens to $\Omega_{k0} = 0.139^{+0.061}_{-0.058}$ that is consistent with flat universe at 95% confidence level. The deceleration parameter $q_0 = -0.481^{+0.057}_{-0.054}$ confirms cosmic acceleration with improved precision. The jerk parameter $j_0 = 1.163^{+0.403}_{-0.425}$ remains consistent with the expected standard value within 68% confidence

Dataset	Ω_{k0}	q_0	j_0	s_0
SGL+PantheonPlus	$0.049^{+0.083}_{-0.077}$	$-0.472^{+0.073}_{-0.067}$	$0.774^{+0.705}_{-0.737}$	$-0.749^{+6.995}_{-6.395}$
SGL+Union3	$0.065^{+0.087}_{-0.082}$	$-0.272^{+0.151}_{-0.121}$	$-0.372^{+1.029}_{-1.196}$	$-3.327^{+7.753}_{-4.832}$
SGL+DESY5	$-0.031^{+0.086}_{-0.075}$	$-0.735^{+0.141}_{-0.135}$	$2.248^{+0.857}_{-0.933}$	$-1.113^{+7.250}_{-6.240}$

Table 2: Parameter constraints from SGL combined with different supernova datasets.

level. At the same time, the snap parameter $s_0 = 2.544^{+2.314}_{-2.110}$ shows a tighter constraint compared to the previous case.

For SGL+Union3+DESI-DR2, the curvature is $\Omega_{k0}=0.132^{+0.066}_{-0.062}$, compatible with a flat universe. The Hubble constant $H_0=66.709^{+0.622}_{-0.636}~{\rm km\,s^{-1}\,Mpc^{-1}}$ aligns with recent Planck observations. The deceleration parameter $q_0=-0.324^{+0.085}_{-0.103}$ narrows the allowed range, and the jerk parameter $j_0=0.208^{+0.647}_{-0.488}$ is consistent with standard predictions. The snap parameter $s_0=-1.452^{+2.537}_{-1.214}$ is better constrained compared to the non-DESI case.

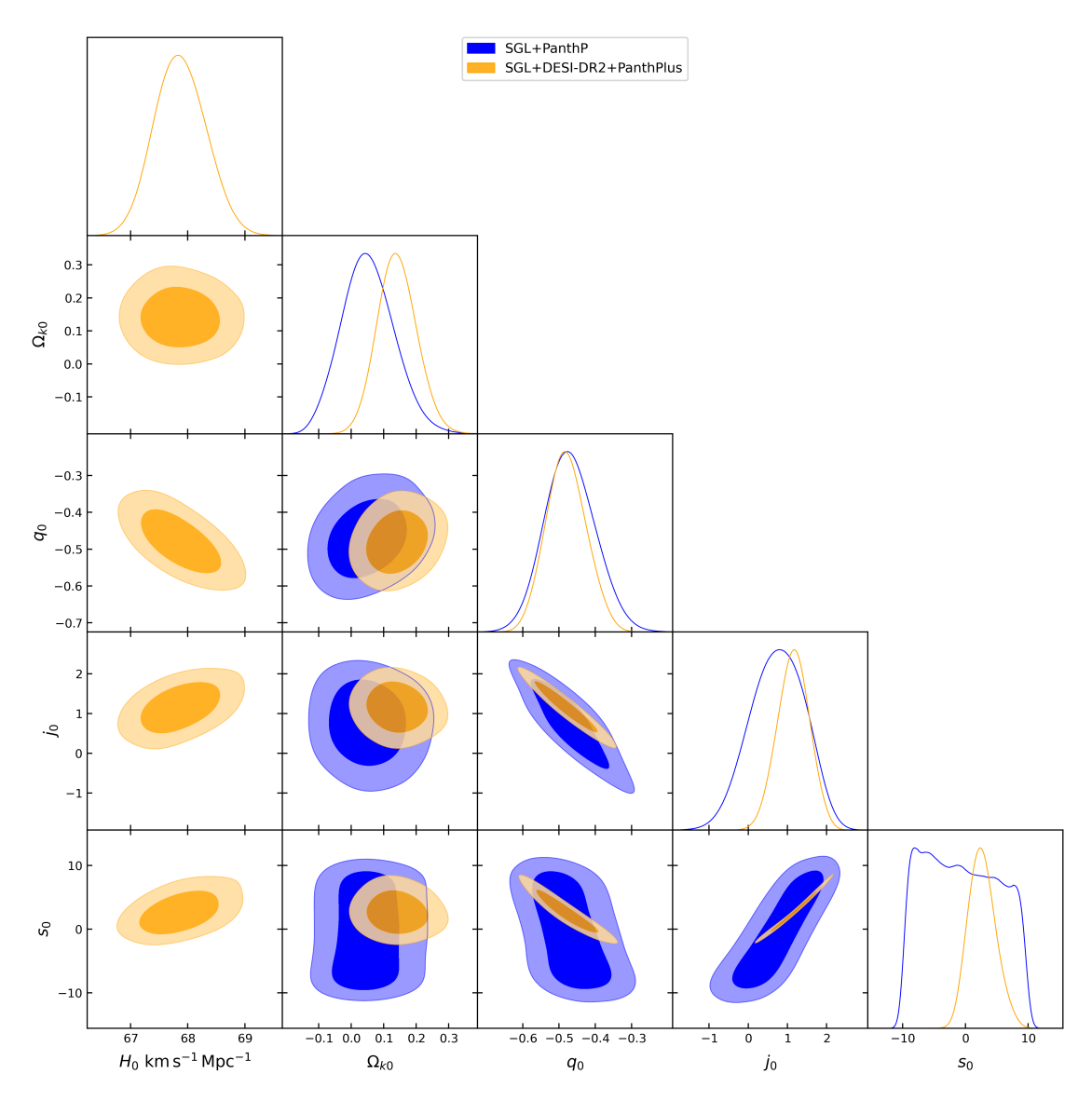
For SGL+DESY5+DESI-DR2, the best-fit value of the curvature, $\Omega_{k0}=-0.054^{+0.050}_{-0.046}$, indicates a slight closed universe while still supporting a flat geometry within the 95% confidence level. The deceleration parameter $q_0=-0.546^{+0.087}_{-0.081}$ agrees with an accelerating universe, and the jerk parameter $j_0=1.344^{+0.628}_{-0.616}$ overlaps with the standard model expectation. The snap parameter $s_0=3.335^{+3.951}_{-3.191}$ has broad uncertainties but still provides valuable constraints.

Dataset	H_0	Ω_{k0}	q_0	j_0	s_0
SGL+PantheonPlus +DESI-DR2	$67.859^{+0.469}_{-0.438}$	$0.139^{+0.061}_{-0.058}$	$-0.481^{+0.057}_{-0.054}$	$1.163^{+0.403}_{-0.425}$	$2.544^{+2.314}_{-2.110}$
SGL+Union3 +DESI-DR2	$66.709^{+0.622}_{-0.636}$	$0.132^{+0.066}_{-0.062}$	$-0.324^{+0.085}_{-0.103}$	$0.208^{+0.647}_{-0.488}$	$-1.452^{+2.537}_{-1.214}$
SGL+DESY5 +DESI-DR2	$68.720^{+0.520}_{-0.633}$	$-0.054^{+0.050}_{-0.046}$	$-0.546^{+0.087}_{-0.081}$	$1.344^{+0.628}_{-0.616}$	$3.335^{+3.951}_{-3.191}$

Table 3: Parameter constraints from SGL combined with different supernova datasets including DESI-DR2.

3.3 Contour Analysis and Parameter Dependencies

Figures 1, 2, and 3 show the joint posterior distributions with 68% and 95% confidence regions for the considered parameters. These figures clearly demonstrate the impact of DESI-DR2 on tightening the constraints and reducing parameter uncertainties.



(a) Joint 68% and 95% confidence contours and posterior distributions using SGL+PantheonPlus and SGL+PantheonPlus+DESI-DR2 datasets.

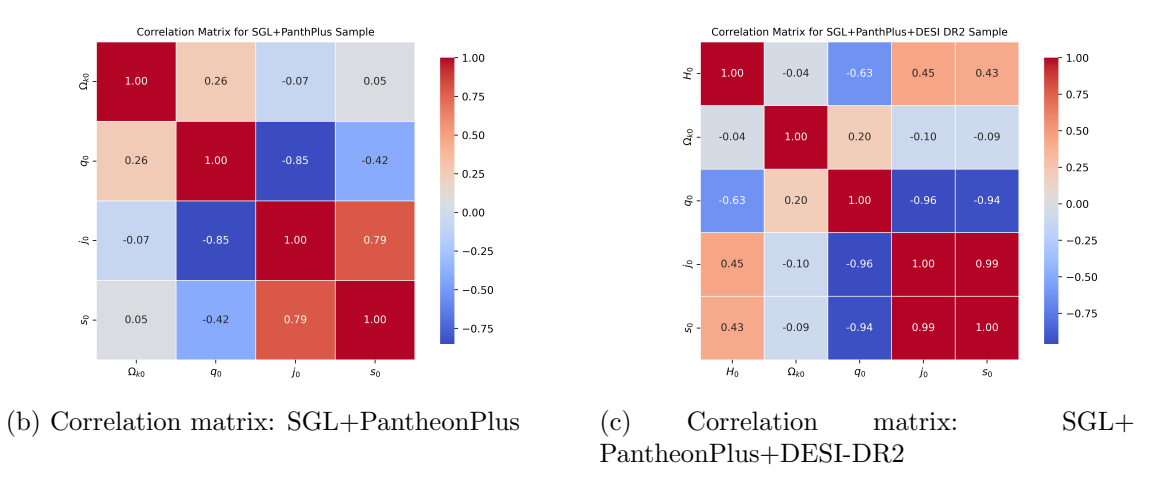
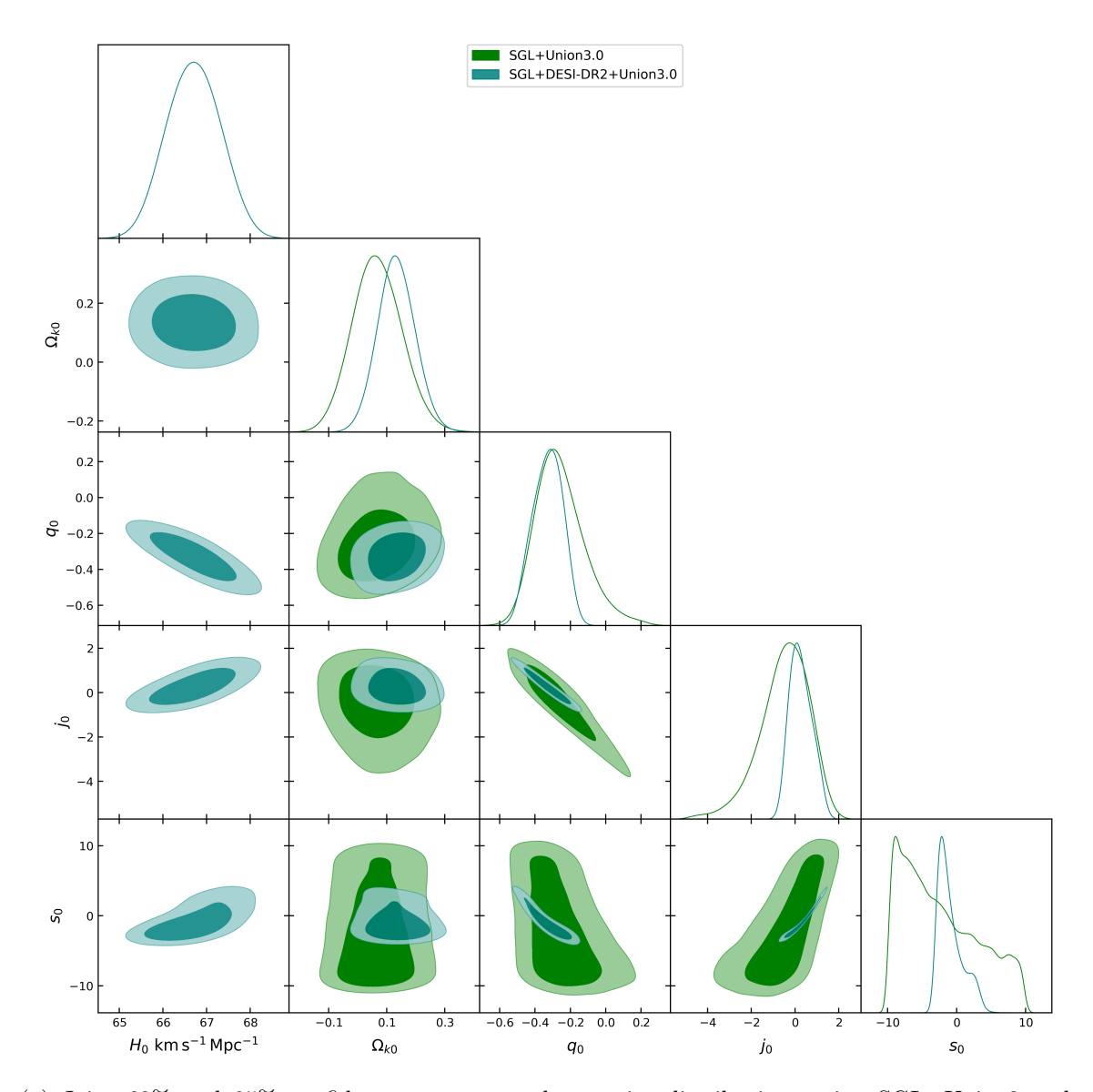


Figure 1: (a) Posterior contours for SGL+PentheonPlus and SGL+PentheonPlus+DESI-DR2 datasets; (b)–(c) corresponding correlation matrices for each dataset combination.



(a) Joint 68% and 95% confidence contours and posterior distributions using SGL+Union3 and SGL+Union3+DESI-DR2 datasets.

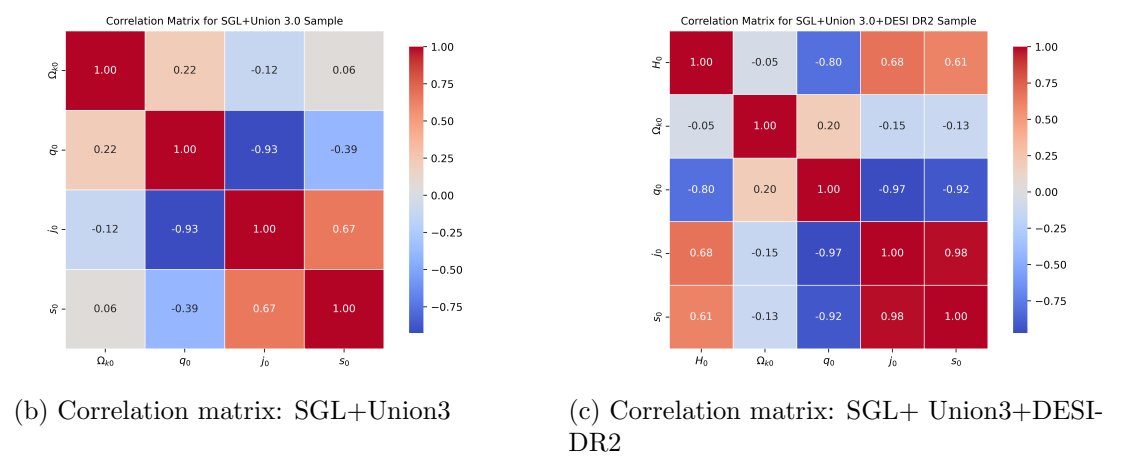
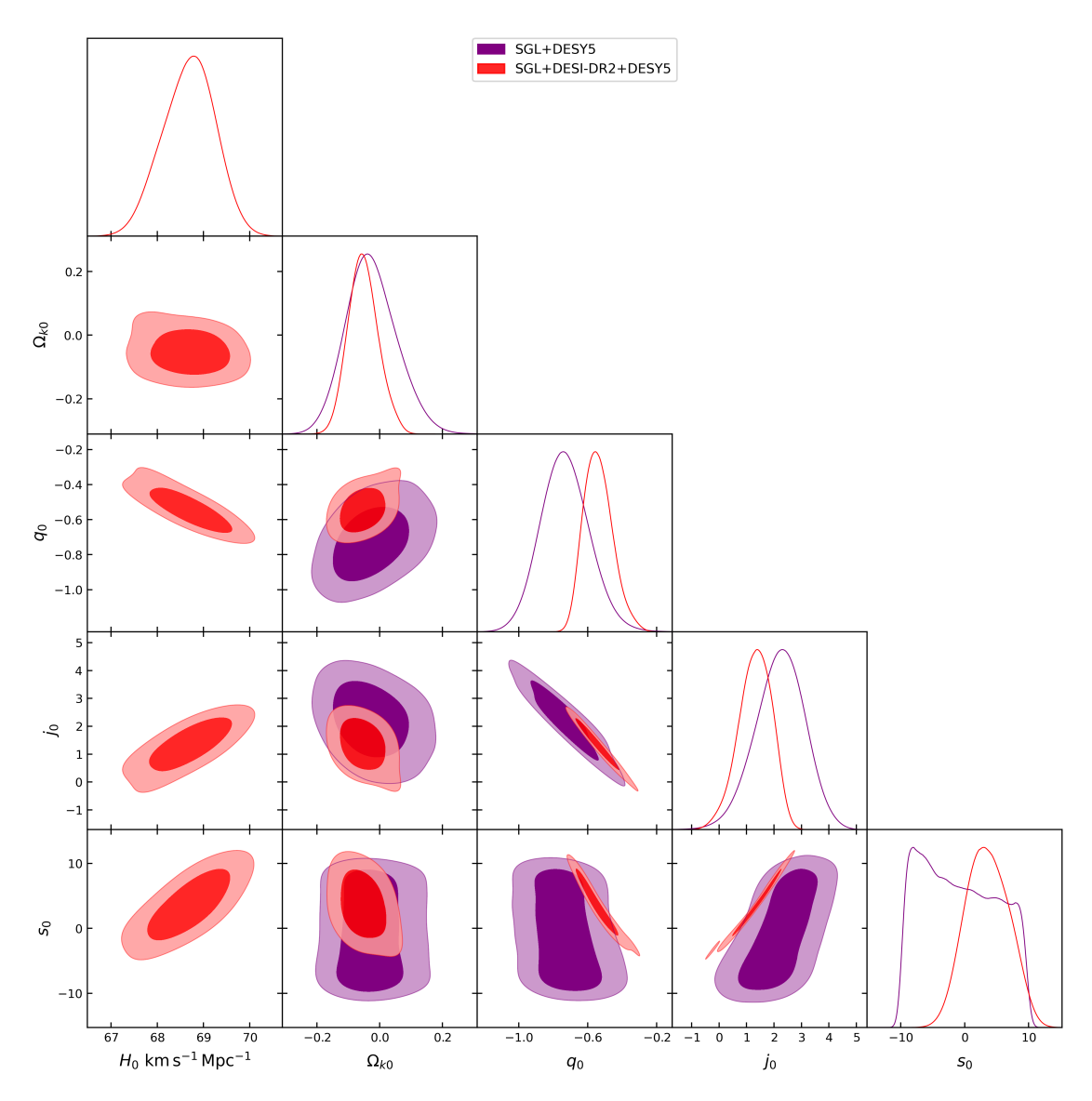


Figure 2: (a) Posterior contours for SGL+Union3 and SGL+Union3+DESI-DR2 datasets; (b)–(c) corresponding correlation matrices for each dataset combination.



(a) Joint 68% and 95% confidence contours and posterior distributions using SGL+DESY5 and SGL+DESY5+DESI-DR2 datasets.

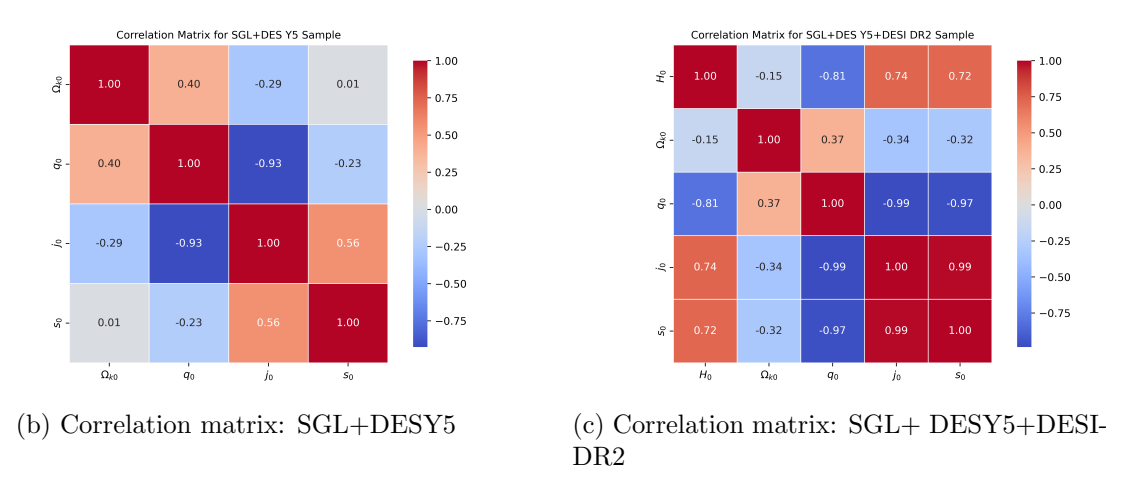


Figure 3: (a) Posterior contours for SGL+DESY5 and SGL+DESY5+DESI-DR2 datasets; (b)–(c) corresponding correlation matrices for each dataset combination.

Figure 1 shows that, for the PantheonPlus dataset, the constraints improve significantly with DESI-DR2. The contours for Ω_{k0} and the cosmographic parameters shrink, and this shows a better determination of these parameters.

Figure 2 presents a similar trend for the Union3 dataset, where the contours without DESI-DR2 exhibit substantial degeneracies between curvature and deceleration. With DESI-DR2, the contours contract and overlap more closely with the expectations from a flat universe.

Figure 3 confirms that, even for the DESY5 sample, which shows broader constraints without DESI, the inclusion of DESI-DR2 markedly enhances the precision of all parameters. The tighter contours for Ω_{k0} and q_0 further support the consistency with the Λ CDM model.

The results show that including DESI-DR2 in cosmographic analyses tightens parameter constraints, improves agreement with standard cosmology, and reduces uncertainties across multiple observational probes.

4 Discussions and Conclusions

In this work, we perform a cosmographic investigation by utilizing strong gravitational lensing distance ratios in conjunction with Type Ia supernova datasets and the DESI-DR2 compilation. Our goal is to refine the estimates of cosmological parameters, including the Hubble constant (H_0) , spatial curvature parameter (Ω_{k0}) , deceleration parameter (q_0) , jerk parameter (j_0) , and snap parameter (s_0) , by performing an analysis that combines diverse observational probes. To put constraints on cosmological parameters, we use Bayesian inference with Markov Chain Monte Carlo (MCMC) methods, marginalize over nuisance parameters, and quantify the confidence regions. Compared with previous studies, this analysis introduces novel ways to assess cosmographic parameters by combining distance ratios from SGL with independent supernova measurements, thereby reducing reliance on traditional distance ladders.

Earlier cosmographic analyses predominantly emphasized distance measurements such as baryon acoustic oscillations or supernova compilations [72, 73], while other works incorporated the distance sum rule (DSR) to constrain curvature using heterogeneous datasets [10, 74]. Although some efforts incorporated strong lensing observations, they often depended on calibrated distance measures rooted in local observations [9, 75]. Our approach uniquely combines the distance sum rule with cosmographic expansions and SGL distance ratios, supported by DESI-DR2 data, to construct an independent and robust estimation of the universe's expansion geometry. This methodology improves the precision and model-testing capabilities by offering a complementary dataset-based approach that mitigates systematic dependencies.

This paper is the second in a two-part study that explores cosmographic constraints from strong gravitational lensing and related datasets. **Paper I** examined time-delay systems and showed that DESI-DR2 changes the curvature preference: the sign of Ω_{k0} shifted from positive to negative once DESI-DR2 was included. That analysis also made clear that the observed shift arises from a degeneracy between curvature and late-time expansion. The present paper builds on those results and studies lensing distance ratios, which do not involve H_0 as a free

parameter. This feature sets them apart from time-delay systems and makes them directly sensitive to curvature and higher-order cosmographic parameters. The combination of these two studies provides complementary tests; time delays set the absolute distance scale, and distance ratios probe the relative geometry, and thus offers a more complete view of late-time cosmology. The primary conclusions of our study are summarized as follows:

- Analysis without DESI-DR2: The constraints derived from combining SGL with individual supernova samples such as PantheonPlus, Union3, and DESY5 remain broad, particularly for higher-order cosmographic parameters. The inferred values of H_0 tend to exceed those predicted by Planck's Λ CDM results ($H_0 \approx 67.4 \,\mathrm{km\,s^{-1}\,Mpc^{-1}}$), though within obtained error values. The curvature parameter Ω_{k0} shows hints of deviation but does not significantly contradict flat geometry. The deceleration parameter q_0 is less negative, suggesting weaker cosmic acceleration. Uncertainties in j_0 and s_0 are considerable, with s_0 being poorly constrained. The inclusion of distance ratio samples of SGL helps stabilize parameter estimation but cannot fully overcome the statistical limitations posed by the supernova datasets alone.
- Impact of DESI-DR2: The integration of DESI-DR2 data substantially improves parameter constraints. The uncertainties shrink by multiple factors, and parameter estimates for H_0 align more closely with the standard cosmological model. The curvature parameter is tightly clustered around zero, and the deceleration parameter conforms to expectations of an accelerating universe. The jerk parameter approaches its standard theoretical value, and even the higher-order snap parameter benefits from the additional data, becoming more constrained. The inclusion of DESI-DR2 helps in reduce uncertainties and improves the robustness of the cosmographic results.
- Comparison with Λ CDM: Without DESI-DR2, the estimates of q_0 and s_0 show larger uncertainties in q_0 and s_0 parameters. These differences become smaller when DESI-DR2 data are added. The tension matrix in Figure 4 shows the level of deviation from the reference values for different dataset combinations. The results show that the differences seen without DESI-DR2 mainly come from limited statistical precision and not from any real inconsistency in the cosmological model.
- Parameter Constraints and Improvements: The analysis of the joint likelihoods reveals that the parameter space shows large, weakly constrained contours when DESI-DR2 is excluded. This is particularly evident for the parameter Ω_{k0} and cosmographic parameters, where the extended contours impose fundamental limits on the precision of any resulting constraints. The inclusion of the DESI-DR2 dataset dramatically reduces the area of these contours and produces tightly defined confidence regions. The correlation matrices (Figures 1, 2, and 3) further reveal a modest rise in the correlations among the cosmographic parameters themselves. This pattern signifies that the dataset requires a more coherent and unified constraint across the entire parameter space. This overall refinement is supported by the distance ratios, which improves the stability and precision of the cosmographic inferences. The consistency between the tightened contours and the correlation matrices offers a unified view of the significant improvement achieved by including DESI-DR2.

While our results offer valuable perspective into cosmographic parameter estimation, it is essential to recognize the limitations inherent in the datasets and methodology. Sys-

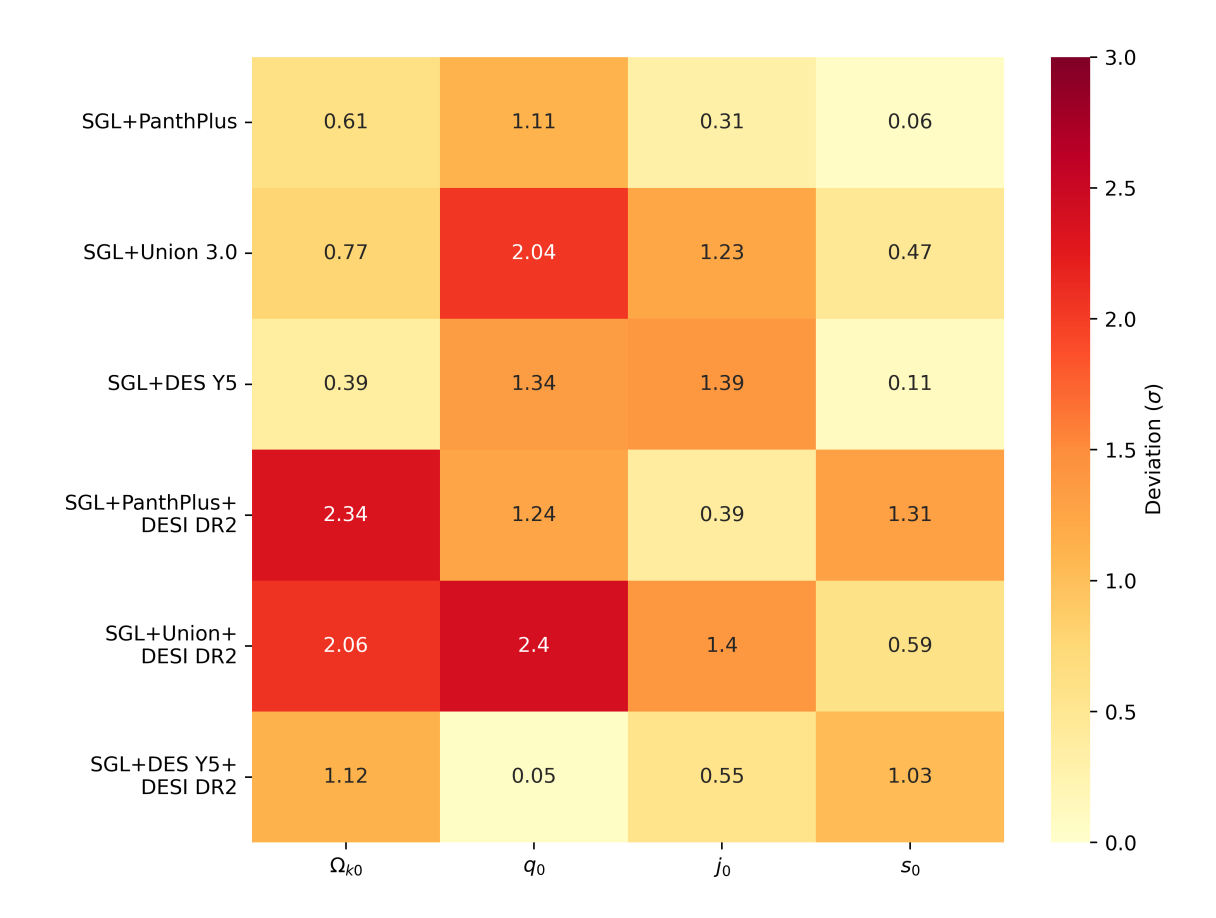


Figure 4: Tension matrix displaying the deviation from the reference values ($\Omega_{k0} = 0$, $q_0 = -0.55$, $j_0 = 1$, $s_0 = -0.35$) in units of σ for various observational combinations. The results highlight how the inclusion of DESI-DR2 data systematically reduces deviations, especially for higher-order cosmographic parameters.

tematic effects arising from lens mass modeling, environmental contamination, or selection biases in supernova surveys may introduce uncertainties. Furthermore, the significant error bars in parameters such as j_0 and s_0 suggest that current datasets, although informative, are not sufficient to fully characterize higher-order dynamics in the universe's expansion. Future analyses should incorporate refined modeling approaches and extended datasets to better isolate these effects and ensure reliability.

For future work, several directions can further enhance the cosmographic framework. Incorporating additional datasets such as baryon acoustic oscillations, cosmic chronometers, and weak lensing observations would provide complementary constraints and reduce degeneracies. It will be critical for future precision cosmology to better understand and mitigate systematic uncertainties, particularly in lens modeling and supernova calibration. It is also possible that the exploration of extended cosmographic formulations or alternative gravity theories will provide a deeper understanding of dark energy and cosmic acceleration. The application of sophisticated statistical techniques, including machine learning algorithms, may also prove instrumental in handling complex parameter spaces and extracting robust

constraints.

In conclusion, our analysis demonstrates that the integration of strong lensing distance ratios with supernova observations, especially when supplemented by DESI-DR2 data, produces tighter and more consistent cosmographic constraints. These results not only support the standard Λ CDM model but also establish a framework for future explorations into the universe's expansion history. The methodology developed here sets the way for more accurate and independent assessments of cosmological parameters, thus laying the groundwork for upcoming observational datasets and theoretical advancements.

Acknowledgments

Darshan Kumar is supported by the Startup Research Fund of the Henan Academy of Sciences, China under Grant number 241841219. One of the authors (Deepak Jain) thanks Inter-University Centre for Astronomy and Astrophysics (IUCAA), Pune (India) for the hospitality provided under the associateship programme where part of the work was done. In this work the figures were created with GetDist [76], numpy [77] and matplotlib [78] Python modules and to estimate parameters we used the publicly available MCMC algorithm emcee [79].

References

- Planck Collaboration, N. Aghanim, Y. Akrami, M. Ashdown, J. Aumont, C. Baccigalupi et al., *Planck 2018 results. VI. Cosmological parameters, Astron. Astrophys.* 641 (2020) A6 [1807.06209].
- [2] A.G. Riess, W. Yuan, L.M. Macri, D. Scolnic, D. Brout, S. Casertano et al., A Comprehensive Measurement of the Local Value of the Hubble Constant with 1 km s⁻¹ Mpc⁻¹ Uncertainty from the Hubble Space Telescope and the SH0ES Team, Astrophys. J. Lett. 934 (2022) L7 [2112.04510].
- [3] E. Di Valentino, A. Melchiorri and J. Silk, *Planck evidence for a closed Universe and a possible crisis for cosmology*, *Nature Astronomy* 4 (2020) 196 [1911.02087].
- [4] W. Handley, Curvature tension: Evidence for a closed universe, Phys. Rev. D 103 (2021) L041301 [1908.09139].
- [5] S. Weinberg, The cosmological constant problem, Reviews of Modern Physics 61 (1989) 1.
- [6] I. Zlatev, L. Wang and P.J. Steinhardt, Quintessence, Cosmic Coincidence, and the Cosmological Constant, Phys. Rev. Lett. 82 (1999) 896 [astro-ph/9807002].
- [7] S. Weinberg, The Cosmological Constant Problems (Talk given at Dark Matter 2000, February, 2000), arXiv e-prints (2000) astro [astro-ph/0005265].
- [8] S. Räsänen, K. Bolejko and A. Finoguenov, New Test of the Friedmann-Lemaître-Robertson-Walker Metric Using the Distance Sum Rule, Phys. Rev. Lett. 115 (2015) 101301 [1412.4976].
- [9] T. Collett, F. Montanari and S. Räsänen, Model-Independent Determination of H_0 and Ω_{K0} from Strong Lensing and Type Ia Supernovae, Phys. Rev. Lett. 123 (2019) 231101 [1905.09781].
- [10] S.-S. Du, J.-J. Wei, Z.-Q. You, Z.-C. Chen, Z.-H. Zhu and E.-W. Liang, Model-independent determination of H_0 and $\Omega_{K,0}$ using time-delay galaxy lenses and gamma-ray bursts, Mon. Not. R. Astron. Soc. **521** (2023) 4963 [2302.13887].

- [11] K. Liao, Constraints on cosmic curvature with lensing time delays and gravitational waves, Phys. Rev. D 99 (2019) 083514 [1904.01744].
- [12] T. Treu, Strong Lensing by Galaxies, Ann. Rev. Astron. Astrophys. 48 (2010) 87 [1003.5567].
- [13] S. Refsdal, On the possibility of determining Hubble's parameter and the masses of galaxies from the gravitational lens effect, Mon. Not. R. Astron. Soc. 128 (1964) 307.
- [14] S. Birrer, M. Millon, D. Sluse, A.J. Shajib, F. Courbin, S. Erickson et al., Time-Delay Cosmography: Measuring the Hubble Constant and Other Cosmological Parameters with Strong Gravitational Lensing, Space Sci. Rev. 220 (2024) 48 [2210.10833].
- [15] T. Treu and L.V.E. Koopmans, The Internal Structure and Formation of Early-Type Galaxies: The Gravitational Lens System MG 2016+112 at z = 1.004, Astrophys. J. 575 (2002) 87 [astro-ph/0202342].
- [16] L.V.E. Koopmans and T. Treu, The Structure and Dynamics of Luminous and Dark Matter in the Early-Type Lens Galaxy of 0047-281 at z = 0.485, Astrophys. J. **583** (2003) 606 [astro-ph/0205281].
- [17] L.V.E. Koopmans, T. Treu, A.S. Bolton, S. Burles and L.A. Moustakas, The Sloan Lens ACS Survey. III. The Structure and Formation of Early-Type Galaxies and Their Evolution since z ~1, Astrophys. J. 649 (2006) 599 [astro-ph/0601628].
- [18] S. Cao, Z.-H. Zhu and R. Zhao, Testing and selecting dark energy models with lens redshift data, Phys. Rev. D 84 (2011) 023005.
- [19] M. Biesiada, A. Piórkowska and B. Malec, Cosmic equation of state from strong gravitational lensing systems, Mon. Not. R. Astron. Soc. 406 (2010) 1055 [1105.0946].
- [20] Y.-J. Wang, J.-Z. Qi, B. Wang, J.-F. Zhang, J.-L. Cui and X. Zhang, Cosmological model-independent measurement of cosmic curvature using distance sum rule with the help of gravitational waves, Mon. Not. R. Astron. Soc. 516 (2022) 5187 [2201.12553].
- [21] A. Rana, D. Jain, S. Mahajan and A. Mukherjee, Constraining cosmic curvature by using age of galaxies and gravitational lenses, J. Cosmol. Astropart. Phys. **03** (2017) 028 [1611.07196].
- [22] S. Cao, M. Biesiada, R. Gavazzi, A. Piórkowska and Z.-H. Zhu, Cosmology with Strong-lensing Systems, Astrophys. J. 806 (2015) 185 [1509.07649].
- [23] X.-L. Li, S. Cao, X.-G. Zheng, S. Li and M. Biesiada, Comparison of cosmological models using standard rulers and candles, Research in Astronomy and Astrophysics 16 (2016) 84 [1510.03494].
- [24] S. Cao, M. Biesiada, M. Yao and Z.-H. Zhu, Limits on the power-law mass and luminosity density profiles of elliptical galaxies from gravitational lensing systems, Mon. Not. R. Astron. Soc. 461 (2016) 2192 [1604.05625].
- [25] J.-L. Cui, H.-L. Li and X. Zhang, No evidence for the evolution of mass density power-law index γ from strong gravitational lensing observation, Science China Physics, Mechanics, and Astronomy 60 (2017) 80411 [1704.07614].
- [26] Y. Chen, R. Li, Y. Shu and X. Cao, Assessing the effect of lens mass model in cosmological application with updated galaxy-scale strong gravitational lensing sample, Mon. Not. R. Astron. Soc. 488 (2019) 3745 [1809.09845].
- [27] J.-Q. Xia, H. Yu, G.-J. Wang, S.-X. Tian, Z.-X. Li, S. Cao et al., Revisiting Studies of the Statistical Property of a Strong Gravitational Lens System and Model-Independent Constraint on the Curvature of the Universe, Astrophys. J. 834 (2017) 75 [1611.04731].
- [28] T. Li, T.E. Collett, C.M. Krawczyk and W. Enzi, Cosmology from large populations of galaxy-galaxy strong gravitational lenses, Mon. Not. R. Astron. Soc. 527 (2024) 5311 [2307.09271].

- [29] S. Guerrini and E. Mörtsell, Probing a scale dependent gravitational slip with galaxy strong lensing systems, Phys. Rev. D 109 (2024) 023533 [2309.11915].
- [30] S. Weinberg, Gravitation and Cosmology: Principles and Applications of the General Theory of Relativity (1972).
- [31] M. Visser, Energy conditions in the epoch of galaxy formation., Science 276 (1997) 88 [1501.01619].
- [32] M. Visser, Cosmography: Cosmology without the Einstein equations, General Relativity and Gravitation 37 (2005) 1541.
- [33] R.R. Caldwell and M. Kamionkowski, Expansion, geometry, and gravity, J. Cosmol. Astropart. Phys. 09 (2004) 009 [astro-ph/0403003].
- [34] A.G. Riess, L.-G. Strolger, J. Tonry, S. Casertano, H.C. Ferguson, B. Mobasher et al., Type Ia Supernova Discoveries at z & 1 from the Hubble Space Telescope: Evidence for Past Deceleration and Constraints on Dark Energy Evolution, Astrophys. J. 607 (2004) 665 [astro-ph/0402512].
- [35] M. Chevallier and D. Polarski, Accelerating Universes with Scaling Dark Matter, International Journal of Modern Physics D 10 (2001) 213 [gr-qc/0009008].
- [36] E.V. Linder, Exploring the Expansion History of the Universe, Phys. Rev. Lett. **90** (2003) 091301 [astro-ph/0208512].
- [37] C. Gruber and O. Luongo, Cosmographic analysis of the equation of state of the universe through Padé approximations, Phys. Rev. D 89 (2014) 103506 [1309.3215].
- [38] A. Shafieloo, Crossing statistic: Bayesian interpretation, model selection and resolving dark energy parametrization problem, J. Cosmol. Astropart. Phys. **05** (2012) 024 [1202.4808].
- [39] R.D. Blandford and R. Narayan, Cosmological applications of gravitational lensing., Ann. Rev. Astron. Astrophys. 30 (1992) 311.
- [40] R. Narayan and M. Bartelmann, Lectures on Gravitational Lensing, arXiv e-prints (1996) astro [astro-ph/9606001].
- [41] I. Jorgensen, M. Franx and P. Kjaergaard, Spectroscopy for E and S0 galaxies in nine clusters, Mon. Not. R. Astron. Soc. 276 (1995) 1341.
- [42] M. Cappellari, R. Bacon, M. Bureau, M.C. Damen, R.L. Davies, P.T. de Zeeuw et al., The SAURON project - IV. The mass-to-light ratio, the virial mass estimator and the Fundamental Plane of elliptical and lenticular galaxies, Mon. Not. R. Astron. Soc. 366 (2006) 1126 [astro-ph/0505042].
- [43] L.V.E. Koopmans and T. Treu, The Stellar Velocity Dispersion of the Lens Galaxy in MG 2016+112 at z=1.004, Astrophys. J. Lett. 568 (2002) L5 [astro-ph/0201017].
- [44] T. Treu and L.V.E. Koopmans, Massive Dark Matter Halos and Evolution of Early-Type Galaxies to z ~1, Astrophys. J. 611 (2004) 739 [astro-ph/0401373].
- [45] A.J. Ruff, R. Gavazzi, P.J. Marshall, T. Treu, M.W. Auger and F. Brault, The SL2S Galaxy-scale Lens Sample. II. Cosmic Evolution of Dark and Luminous Mass in Early-type Galaxies, Astrophys. J. 727 (2011) 96 [1008.3167].
- [46] A. Sonnenfeld, R. Gavazzi, S.H. Suyu, T. Treu and P.J. Marshall, The SL2S Galaxy-scale Lens Sample. III. Lens Models, Surface Photometry, and Stellar Masses for the Final Sample, Astrophys. J. 777 (2013) 97 [1307.4764].
- [47] A. Sonnenfeld, T. Treu, R. Gavazzi, S.H. Suyu, P.J. Marshall, M.W. Auger et al., The SL2S Galaxy-scale Lens Sample. IV. The Dependence of the Total Mass Density Profile of Early-type Galaxies on Redshift, Stellar Mass, and Size, Astrophys. J. 777 (2013) 98 [1307.4759].

- [48] A. Sonnenfeld, T. Treu, P.J. Marshall, S.H. Suyu, R. Gavazzi, M.W. Auger et al., The SL2S Galaxy-scale Lens Sample. V. Dark Matter Halos and Stellar IMF of Massive Early-type Galaxies Out to Redshift 0.8, Astrophys. J. 800 (2015) 94 [1410.1881].
- [49] A.S. Bolton, S. Burles, L.V.E. Koopmans, T. Treu, R. Gavazzi, L.A. Moustakas et al., The Sloan Lens ACS Survey. V. The Full ACS Strong-Lens Sample, Astrophys. J. 682 (2008) 964 [0805.1931].
- [50] M.W. Auger, T. Treu, A.S. Bolton, R. Gavazzi, L.V.E. Koopmans, P.J. Marshall et al., The Sloan Lens ACS Survey. IX. Colors, Lensing, and Stellar Masses of Early-Type Galaxies, Astrophys. J. 705 (2009) 1099 [0911.2471].
- [51] M.W. Auger, T. Treu, A.S. Bolton, R. Gavazzi, L.V.E. Koopmans, P.J. Marshall et al., The Sloan Lens ACS Survey. X. Stellar, Dynamical, and Total Mass Correlations of Massive Early-type Galaxies, Astrophys. J. 724 (2010) 511 [1007.2880].
- [52] Y. Shu, A.S. Bolton, J.R. Brownstein, A.D. Montero-Dorta, L.V.E. Koopmans, T. Treu et al., The Sloan Lens ACS Survey. XII. Extending Strong Lensing to Lower Masses, Astrophys. J. 803 (2015) 71 [1407.2240].
- [53] Y. Shu, J.R. Brownstein, A.S. Bolton, L.V.E. Koopmans, T. Treu, A.D. Montero-Dorta et al., The Sloan Lens ACS Survey. XIII. Discovery of 40 New Galaxy-scale Strong Lenses, Astrophys. J. 851 (2017) 48 [1711.00072].
- [54] J.R. Brownstein, A.S. Bolton, D.J. Schlegel, D.J. Eisenstein, C.S. Kochanek, N. Connolly et al., The BOSS Emission-Line Lens Survey (BELLS). I. A Large Spectroscopically Selected Sample of Lens Galaxies at Redshift ~0.5, Astrophys. J. 744 (2012) 41 [1112.3683].
- [55] Y. Shu, A.S. Bolton, C.S. Kochanek, M. Oguri, I. Pérez-Fournon, Z. Zheng et al., The BOSS Emission-line Lens Survey. III. Strong Lensing of Lyα Emitters by Individual Galaxies, Astrophys. J. 824 (2016) 86 [1604.01842].
- [56] Y. Shu, A.S. Bolton, S. Mao, C.S. Kochanek, I. Pérez-Fournon, M. Oguri et al., The BOSS Emission-line Lens Survey. IV. Smooth Lens Models for the BELLS GALLERY Sample, Astrophys. J. 833 (2016) 264 [1608.08707].
- [57] K. Lodha et al., Extended Dark Energy analysis using DESI DR2 BAO measurements, arXiv e-prints (2025) arXiv:2503.14743 [2503.14743].
- [58] M. Abdul Karim et al., DESI DR2 Results II: Measurements of Baryon Acoustic Oscillations and Cosmological Constraints, arXiv e-prints (2025) arXiv:2503.14738 [2503.14738].
- [59] B. Bassett and R. Hlozek, Baryon acoustic oscillations, in Dark Energy, P. Ruiz-Lapuente, ed., p. 246 (2010), DOI.
- [60] D.J. Eisenstein and W. Hu, Baryonic Features in the Matter Transfer Function, Astrophys. J. 496 (1998) 605 [astro-ph/9709112].
- [61] R.A. Sunyaev and Y.B. Zeldovich, The Observations of Relic Radiation as a Test of the Nature of X-Ray Radiation from the Clusters of Galaxies, Comments on Astrophysics and Space Physics 4 (1972) 173.
- [62] A.G. Adame et al., DESI 2024 VI: cosmological constraints from the measurements of baryon acoustic oscillations, J. Cosmol. Astropart. Phys. **02** (2025) 021 [2404.03002].
- [63] D. Scolnic, D. Brout, A. Carr, A.G. Riess, T.M. Davis, A. Dwomoh et al., The Pantheon+ Analysis: The Full Data Set and Light-curve Release, Astrophys. J. 938 (2022) 113 [2112.03863].
- [64] D. Rubin, G. Aldering, M. Betoule, A. Fruchter, X. Huang, A.G. Kim et al., Union through UNITY: Cosmology with 2000 SNe Using a Unified Bayesian Framework, Astrophys. J. 986 (2025) 231 [2311.12098].

- [65] DES Collaboration, T.M.C. Abbott, M. Acevedo, M. Aguena, A. Alarcon, S. Allam et al., The Dark Energy Survey: Cosmology Results with ~1500 New High-redshift Type Ia Supernovae Using the Full 5 yr Data Set, Astrophys. J. Lett. 973 (2024) L14 [2401.02929].
- [66] D. Brout, D. Scolnic, R. Kessler, C.B. D'Andrea, T.M. Davis, R.R. Gupta et al., First Cosmology Results Using SNe Ia from the Dark Energy Survey: Analysis, Systematic Uncertainties, and Validation, Astrophys. J. 874 (2019) 150 [1811.02377].
- [67] D. Brout and D. Scolnic, It's Dust: Solving the Mysteries of the Intrinsic Scatter and Host-galaxy Dependence of Standardized Type Ia Supernova Brightnesses, Astrophys. J. 909 (2021) 26 [2004.10206].
- [68] B. Popovic, D. Brout, R. Kessler, D. Scolnic and L. Lu, Improved Treatment of Host-galaxy Correlations in Cosmological Analyses with Type Ia Supernovae, Astrophys. J. 913 (2021) 49 [2102.01776].
- [69] B. Popovic, D. Brout, R. Kessler and D. Scolnic, The Pantheon+ Analysis: Forward Modeling the Dust and Intrinsic Color Distributions of Type Ia Supernovae, and Quantifying Their Impact on Cosmological Inferences, Astrophys. J. 945 (2023) 84 [2112.04456].
- [70] G. Jiang and C.S. Kochanek, The Baryon Fractions and Mass-to-Light Ratios of Early-Type Galaxies, Astrophys. J. 671 (2007) 1568 [0705.3647].
- [71] D. Foreman-Mackey, D.W. Hogg, D. Lang and J. Goodman, emcee: The MCMC Hammer, 1202.3665.
- [72] V. Vitagliano, J.-Q. Xia, S. Liberati and M. Viel, High-redshift cosmography, J. Cosmol. Astropart. Phys. 03 (2010) 005 [0911.1249].
- [73] M. Rezaei, S. Pour-Ojaghi and M. Malekjani, A Cosmography Approach to Dark Energy Cosmologies: New Constraints Using the Hubble Diagrams of Supernovae, Quasars, and Gamma-Ray Bursts, Astrophys. J. 900 (2020) 70 [2008.03092].
- [74] J.-Z. Qi, S. Cao, S. Zhang, M. Biesiada, Y. Wu and Z.-H. Zhu, The distance sum rule from strong lensing systems and quasars - test of cosmic curvature and beyond, Mon. Not. R. Astron. Soc. 483 (2019) 1104 [1803.01990].
- [75] D. Kumar, D. Jain, S. Mahajan, A. Mukherjee and N. Rani, Constraining cosmological and galaxy parameters using strong gravitational lensing systems, Phys. Rev. D 103 (2021) 063511 [2002.06354].
- [76] A. Lewis, GetDist: a Python package for analysing Monte Carlo samples, arXiv e-prints (2019) arXiv:1910.13970 [1910.13970].
- [77] T.E. Oliphant, A guide to numpy, Trelgol Publishing USA 1 (2006).
- [78] J.D. Hunter, Matplotlib: A 2d graphics environment, Comput. Sci. Eng. 9 (2007) 90.
- [79] D. Foreman-Mackey, D.W. Hogg, D. Lang and J. Goodman, emcee: The MCMC Hammer, Publ. Astron. Soc. Pac. 125 (2013) 306 [1202.3665].